Sum Rate Maximization of Full-Duplex MIMO Monostatic Backscatter Networks Under Residual Self-Interference

Azar Hakimi
Faculty of Engineering
University of Alberta
Edmonton, Canada
hakimina@ualberta.ca

Shayan Zargari
Faculty of Engineering
University of Alberta
Edmonton, Canada
zargari@ualberta.ca

Chintha Tellambura
Faculty of Engineering
University of Alberta
Edmonton, Canada
ct4@ualberta.ca

Sanjeewa Herath
Research and Development Centre
Huawei
Ottawa, Canada
sanjeewa.herath@huawei.com

***Abstract*—Backscatter communication (BCS) devices have low cost, low power, and the ability to harvest energy, enabling ultra-green Internet of things (IoT) networks with energy autonomy. However, they achieve only low data rates and a limited communication range. A monostatic backscatter (MBS) network of multiple tags with a full-duplex (FD) multiple-input multiple-output (MIMO) reader is subject to self-interference (SI), which exacerbates the aforementioned problems. Since SI cannot be removed ideally, the residual SI (RSI) degrades the system performance. Thus, the main goal of this study is to correct this problem. To this end, we formulate the maximization of the sum rate by optimizing the precoder and combiner filters of the reader and the reflection coefficients of the tags. The constraints are to limit the effects of the RSI and allow the energy harvested by the tags to exceed a minimum. Because the problem is nonconvex, we utilize alternating optimization (AO) to split it into three subproblems and develop iterative algorithms. The simulation results validate and quantify the achievable sum rate.**

***Index Terms*—Backscatter communication (BSC), residual self-interference (RSI), energy harvesting (EH), full-duplex (FD).**

I. Introduction

For conventional radar applications, Stockman developed backscatter communication (BSC) in 1948 [1]. BSC tags, especially passive ones offer low cost, low power, and the potential to enable self-sustainable communications without or with reduced human intervention. Consequently, BSC networks facilitate sixth-generation (6G) wireless as they enable the internet of things (IoT) and the internet of everything (IoE). Hence, BSC enables many applications including smart homes/cities, healthcare, wearables, radio frequency identification (RFID), and manufacturing applications such as retail, warehouses, and others [2].

The key idea is that the backscatter device (tag) does not generate the radio frequency (RF) carrier [3], avoiding power-hungry RF components. In particular, the tag relies on the incident RF signal to piggyback its data and reflect the signal to the receiver (reader). The RF signal can come from the reader (monostatic BCS), a dedicated server (bistatic BCS), and ambient sources like WiFi or TV tower (ambient BCS). Monostatic BCS eliminates the need for dedicated RF sources and avoids the unpredictability, uncertainty, and interference issues of ambient BCS.

On the other hand, the reader in the monostatic backscatter (MBS) network both transmits and receives simultaneously. Such full-duplex (FD) operation can double the spectral efficiency, reduce the latency, and enhance the communication range [4]. However, the cost of these benefits is self-interference (SI), which can be as high as 110 dB above the desired signal. Surprisingly, previous studies assume assuming perfect self-interference cancellation (SIC). With this assumption, [5]–[7] study optimal transceiver design at the MBS reader and the optimal tag reflection coefficients. Specifically, [5] jointly optimize the downlink energy beamforming, receiving filter at the reader, and tag reflection coefficients. Reference [6] maximizes the minimum rate of the tags to collect data with fairness while considering EH at the tags. With spatial domain multiple access (SDMA), all tags reflect simultaneously. Work [7] derives the capacity lower bound for four different combinations of zero-forcing and matched filter transceiver configurations in a massive multiple-input and multiple-output (MIMO) case and discusses the impact of imperfect channel state information (CSI).

Furthermore, since the tag is a power-limited device, it relies on energy harvesting (EH) to power its operations. Thus, [8]–[11] energy harvesting tags. For example, [8] uses energy beamforming to improve energy transfer efficiency where the energy beamformer maximizes the minimum rate of tags subject to the energy constraint. The reader uses maximum-ratio combining (MRC) and zero-forcing receivers while using the estimated backscatter CSI. Authors in [9] propose an EH-relay network and maximize the system throughput by jointly optimizing the beamforming, power splitting (PS) ratio, and other parameters. Besides, [10] investigates hybrid nodes. The nodes select backscatter or active RF modes depending on ambient RF signals and the amount of harvested energy. Reference [11] studies the energy beamforming using the estimated backscatter CSI and derives optimal resource allocation to maximize the harvested energy at the receivers.

Nevertheless, unlike the previous works [5], [6], we consider

a more realistic model where the analog/digital SIC processes of the reader are not perfect. Thus, non-zero residual self-interference (RSI) will affect the system performance. Thus, we develop the transceiver design for the reader to correct this problem. Specifically, we consider an MBS network with multiple tags and an FD MIMO reader. The reader can utilize the spatial degrees of freedom of MIMO to suppress the effect of RSI while enabling the tags to perform EH. Our contributions are summarized as follows. We maximize the sum rate of the network by jointly optimizing the transmit (precoder) and receive (combiner) beamformers at the reader and the reflection coefficients of the tags subject to the RSI constraint at the reader and EH constraint at the tags. More specifically, this transceiver design satisfies the minimum energy required at the tags and limits the RSI power to a maximum tolerable RSI power, which has been ignored in prior works. The proposed optimization problem is non-convex. We thus exploit the alternating optimization (AO) algorithm to split it into three subproblems. In the first one, we optimize the precoder vector with the help of successive convex approximation (SCA) and semidefinite relaxation (SDR) techniques. In the second subproblem, we derive a closed-form solution for optimal combiner at the reader. The third subproblem optimizes the reflection coefficients of the tags given the solutions of the first two subproblems. We thus solve it with the geometric programming (GP) paradigm. The overall algorithm then iterates until a convergence criterion is met. The numerical results validate its superiority compared to other baselines when RSI power is restricted to be as small as possible.

Notations: Vectors and matrices are expressed by boldface lower case letters $\mathbf{a}$ and capital letters $\mathbf{A}$, respectively. For a square matrix $\mathbf{A}$, $\mathbf{A}^H$, $\mathbf{A}^T$ and $\mathbf{A}^\star$ are Hermitian conjugate transpose, transpose and conjugate of a matrix, respectively. $\mathbf{I}_M$ denotes the M-by-M identity matrix. diag$(\cdot)$ is the diagonalization operation. The Euclidean norm of a complex vector and the absolute value of a complex scalar are denoted by $\|\cdot\|$ and $|\cdot|$, respectively. The distribution of a circularly symmetric complex Gaussian (CSCG) random vector with mean $\boldsymbol{\mu}$ and covariance matrix $\mathbf{C}$ is denoted by $\sim \mathcal{CN}(\boldsymbol{\mu}, \mathbf{C})$. The expectation operator is $\mathbb{E}[\cdot]$. Symbols $\mathcal{C}^{M\times N}$ represents $M \times N$ dimensional complex matrix.

II. System Model

The system model comprises $K \geq 1$ semi-passive single antenna tags indexed by $k \in \mathcal{K} = \{1, \ldots, K\}$, randomly distributed in a $r \times r$ square region, a multiple antenna reader at the center transmits an RF carrier in the downlink while receiving the backscattered signals via the uplink. We denote the k-th tag and the reader as $\mathbf{T_k}$ and $\mathbf{R}$, respectively. We assume the reader is equipped with $N_t \geq 1$ and $N_r \geq 1$ transmit and receive antennas, respectively.

Denote the channels from the $\mathbf{R}$-to-$\mathbf{T_k}$, $\mathbf{T_k}$-to-$\mathbf{R}$, and SI channel as $\mathbf{h}_{T_k}^f \in \mathcal{CN}\left(\mathbf{0}_{N_t\times 1}, \xi_{T_k}^f \mathbf{I}_{N_t}\right)$, $\mathbf{h}_{T_k}^b \in \mathcal{CN}\left(\mathbf{0}_{N_r\times 1}, \xi_{T_k}^b \mathbf{I}_{N_r}\right)$, and $\mathbf{H}_{\text{SI}} = [h_{ij}^{\text{SI}}] \in \mathcal{C}^{N_r\times N_t}$, respectively, where $\xi_{T_k}^f$ and $\xi_{T_k}^b$ indicate the downlink and uplink channels pathloss, respectively. Denote h_{ij}^{SI} the (i,j)-th element of H_{SI}. The SI channel typically is modeled as a Rician fading [12], which consists of two parts: near-field and far-field components represented by the line-of-sight (LOS) and the non-line-of-sight (NLOS) parts. Therefore, the SI channel model is given by

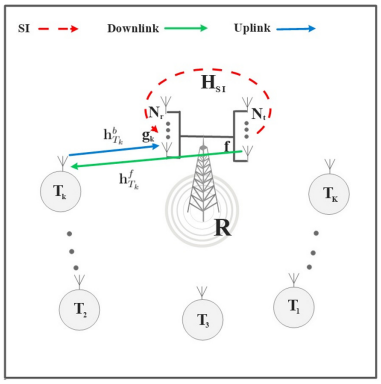

Fig. 1: MBS network with reader ($\mathbf{R}$) and tags ($\mathbf{T_k}$, $k \in \mathcal{K}$).

$$h_{ij}^{\text{SI}} = \sqrt{\frac{1}{\bar{K}+1}} h_{\text{LOS}}^{\text{SI}} + \sqrt{\frac{\bar{K}}{\bar{K}+1}} h_{\text{NLOS}}^{\text{SI}}, \tag{1}$$

where $\bar{K}$ denotes the Rician factor, $h_{\text{LOS}}^{\text{SI}}$ represent the deterministic part subject to $\|h_{\text{LOS}}^{\text{SI}}\|^2 = 1$, and $h_{\text{NLOS}}^{\text{SI}} \sim \mathcal{CN}(0,1)$. Consequently, higher $\bar{K}$ indicates a strong SI channel at the $\mathbf{R}$. We assume a block fading model for all the channels, i.e., the channel remains constant within a coherence time and varies independently between time blocks. Thus, we assume that the reader has full CSI. [1]

Reader $\mathbf{R}$ transmits signal $\mathbf{x} = \sqrt{P_T}\mathbf{f}s$, where P_T is the transmit power, $s \sim \mathcal{CN}(0,1)$ is the $\mathbf{R}$ transmit symbol, and $\mathbf{f} \in \mathcal{C}^{N_t\times 1}$ denotes the precoding vector. It is assumed that the precoder vector is identical for all tags, which is optimal since the transmit signal is only used to power the tag circuits [5]. Consequently, the received signal at $\mathbf{T_k}$, $k \in \mathcal{K}$, can be expressed as $y_{T_k} = (\mathbf{h}_{T_k}^f)^T\mathbf{x}$, $k \in \mathcal{K}$. Each tag modulates its data over the received signal by tuning its load impedance into a number of states to map its data bit on the incident RF signal. Note that since the tag lacks RF components, it does not introduce any noise to the signal. Accordingly, the received signal at the $\mathbf{R}$ is given by

$$\mathbf{y}_R = \sum_{k=1}^{K} \sqrt{\alpha_k}\mathbf{h}_{T_k}^b (\mathbf{h}_{T_k}^f)^T \mathbf{x} b_k + \hat{\mathbf{H}}_{\text{SI}}\mathbf{x} + \mathbf{n}_R, \tag{2}$$

where tag's data symbol b_k, $k \in \mathcal{K}$, satisfies $\mathbb{E}\{|b_k|^2\} = 1$, and $\alpha_k \in [0,1]$ is the reflection coefficient of $\mathbf{T}_k$, $k \in \mathcal{K}$. The first term in (2) is the reflected signals from all tags. The second term denotes the RSI at the $\mathbf{R}$, where $\hat{\mathbf{H}}_{\text{SI}} = \sqrt{\beta}\mathbf{H}_{\text{SI}}$ and $0 \leq \beta \ll 1$ is a constant denoting the SIC ability of

[1] If this assumption is not true due to imperfect CSI, our results serve as theoretical performance upper bounds for the considered FD MIMO BCS network. Robust versions of our algorithms can also be developed to reduce the effect of channel estimation errors.

the $\mathbf{R}$. This factor models the effect of passive/active SIC techniques such as antenna isolation and filtering circuits. The case of $\beta = 0$ denotes the perfect SIC case. Furthermore, $\mathbf{n}_R \sim \mathcal{CN}(\mathbf{0}_{N_r\times 1}, \sigma_R^2\mathbf{I}_{N_r})$ is the additive white Gaussian noise (AWGN) at the $\mathbf{R}$. Indeed, we will refer to β as the hard SI suppression threshold. The smaller β is, the better cancellation is reached. The $\mathbf{R}$ applies the linear detection matrix, i.e., $\mathbf{G} = [\mathbf{g}_1, \dots \mathbf{g}_k, \dots, \mathbf{g}_K] \in \mathcal{C}^{N_r\times K}$, where $\mathbf{g}_k \in \mathcal{C}^{N_r\times 1}$ indicates the combiner vector assigned to $\mathbf{T}_k$, to spatially separate data of all the tags embedded in $\mathbf{y}_R$. Thus, the received SINR at the $\mathbf{R}$ for the k-th data stream from $\mathbf{T}_k$, $k \in \mathcal{K}$, can be written as

$$\gamma_k = \frac{\alpha_k |\mathbf{g}_k^H \mathbf{h}_{T_k}^b|^2 |(\mathbf{h}_{T_k}^f)^T \mathbf{f}|^2}{\sum_{j\neq k}^K \alpha_j |\mathbf{g}_k^H \mathbf{h}_{T_j}^b|^2 |(\mathbf{h}_{T_j}^f)^T \mathbf{f}|^2 + \beta |\mathbf{g}_k^H \mathbf{H}_{\mathrm{SI}} \mathbf{f}|^2 + \frac{\sigma_R^2}{P_T}\|\mathbf{g}_k\|^2}, \tag{3}$$

where the nominator term in (3) is the desired received signal power from $\mathbf{T}_k$, and the denominator comprises the powers of the interference signals, RSI, and noise, respectively. The total sum rate of interest can be expressed as $R_S = \sum_{k=1}^K \log_2(1+\gamma_k)$ [bps/Hz]. However, although the tag's onboard battery can power up its circuits, onboard sensors need continuous power which may deplete the battery of the tag quickly. Hence, EH can compensate for its circuit power consumption if the battery power gets too low. Thus, the amount of harvested energy at $\mathbf{T_k}$, $k \in \mathcal{K}$ can be stated as $\mathrm{P}_{\mathrm{EH}_k} = (1-\alpha_k)\eta P_T |(\mathbf{h}_{T_k}^f)^T \mathbf{f}|^2$, where $\eta \in (0, 1]$ is the efficiency of RF signal to direct current (DC) energy conversion [10].

III. Problem Formulation

Our goal is to maximize the sum rate by jointly optimizing the precoder $\{\mathbf{f}\}$, combiners vectors $\{\mathbf{g}_k\}_{k=1}^K$, and reflection coefficients $\{\alpha_k\}_{k=1}^K$, while maintaining minimum harvested power at each tag and maximum RSI level at the $\mathbf{R}$. As a result, the corresponding optimization problem can be formulated as follows:

$$\begin{aligned}
(\mathrm{P1}): \quad & \max_{\alpha_k, \mathbf{g}_k, \mathbf{f}} \quad R_S, && (4a)\\
& \text{s.t.} \quad \beta |\mathbf{g}_k^H \mathbf{H}_{\mathrm{SI}} \mathbf{f}|^2 \leq \lambda, \ \forall k, && (4b)\\
& \quad \mathrm{P}_{\mathrm{EH}_k} \geq P_{\mathrm{th}}, \ \forall k, && (4c)\\
& \quad 0 < \alpha_k < 1, \ \forall k, && (4d)\\
& \quad \|\mathbf{f}\|^2 = 1, \|\mathbf{g}_k\|^2 = 1, \ \forall k, && (4e)
\end{aligned}$$

where λ and P_{th} denote the software threshold of the RSI and power threshold, respectively. The software threshold refers to the fact that this suppression is done at the signal processing level, which is distinct from the hardware-aided RSI suppression at the $\mathbf{R}$ characterized by β. Constraint (4b) indicates the maximum RSI power level at the $\mathbf{R}$. Constraint (4c) denotes the minimum EH at each tag. Finally, constraints (4d) and (4e) are inherent limits for the reflection coefficients and unit norm of precoding as well as combining vectors, respectively.

IV. Proposed Solution

Problem (P1) is non-convex as the objective function contains entangled terms involving the product of optimization variables. To handle this issue, we resort to the AO algorithm [12]. In the first subproblem, we fix the combining vectors and reflection coefficients and optimize the precoding vector $\mathbf{f}$ by applying the SDR technique and first-order Taylor approximation such that a locally optimal solution can be obtained. In the second subproblem, we fix the precoding vector and reflection coefficients and optimize the combiner. We cast the objective as a generalized Rayleigh quotient, yielding the optimal combiner vector in a closed-form solution. The third subproblem involves optimizing the reflection coefficients. To find a solution, we apply GP, a power control technique [13].

A. Optimization Over $\mathbf{f}$

For given $\mathbf{g}_k$ and α_k, $\forall k \in \mathcal{K}$, the sum rate problem turns into a precoder optimization problem represented as follows:

$$\begin{aligned}
(\mathrm{P2}): \quad & \max_{\mathbf{f}} \quad R_S, && (5a)\\
& \text{s.t.} \quad \beta |\mathbf{g}_k^H \mathbf{H}_{\mathrm{SI}} \mathbf{f}|^2 \leq \lambda, \ \forall k, && (5b)\\
& \quad (1-\alpha_k)\eta |P_T (\mathbf{h}_{T_k}^f)^T \mathbf{f}|^2 \geq P_{\mathrm{th}}, \ \forall k, && (5c)\\
& \quad \|\mathbf{f}\|^2 = 1, \ \forall k. && (5d)
\end{aligned}$$

Generally, the objective function of (P2) is not concave over $\mathbf{f}$. To address this, we apply the SDR technique [12]. Let us define a new optimization variable $\mathbf{F} = \mathbf{f}\mathbf{f}^H$, where matrix $\mathbf{F}$ is semidefinite and satisfies rank-one constraint, i.e., $\mathrm{Rank}(\mathbf{F}) = 1$. Thus, problem (P2) can be reformulated as

$$\begin{aligned}
(\mathrm{P2.1}): \quad & \max_{\mathbf{F}} \quad \Gamma, && (6a)\\
& \text{s.t.} \quad \beta \mathrm{Tr}\left(\mathbf{g}_k^H \mathbf{H}_{\mathrm{SI}} \mathbf{F} \mathbf{H}_{\mathrm{SI}}^H \mathbf{g}_k\right) \leq \lambda, \ \forall k, && (6b)\\
& \quad \mathrm{Tr}\left((\mathbf{h}_{T_k}^f)^T \mathbf{F} \mathbf{h}_{T_k}^f\right) \geq P'_{\mathrm{th}}, \ \forall k, && (6c)\\
& \quad \mathrm{Tr}(\mathbf{F}) = 1, && (6d)\\
& \quad \mathrm{Rank}(\mathbf{F}) = 1, && (6e)
\end{aligned}$$

where $P'_{\mathrm{th}} = \frac{P_{\mathrm{th}}}{(1-\alpha_k)\eta P_T}$ and Γ is given in (7). Problem (P2.1) is still not a convex problem due to constraint (6e). To tackle it, we drop (6e), and resort to the SCA technique by using the first-order Taylor series approximation near a feasible point $\mathbf{F}^o$. Subsequently, (P2.1) is relaxed into

$$\begin{aligned}
(\mathrm{P2.2}): \quad & \max_{\mathbf{F}} \quad \sum_{k=1}^K \log(A_k) - B_k(\mathbf{F}, \mathbf{F}^o), && (8a)\\
& \text{s.t.} \quad \text{(6b)–(6d)}, && (8b)
\end{aligned}$$

where $B_k(\mathbf{F}, \mathbf{F}^o)$ and A_k are given in (9) and (10), respectively. To tighten the obtained upper bound, the feasible solution $\mathbf{F}$ in (P2.2) is updated iteratively by using convex optimization tools such as CVX [14] to find a suboptimal solution. Algorithm 1 details the proposed SCA-based Algorithm, and a similar convergence proof can be found in [12]. Specifically, if $\mathbf{F}^*$ which is the optimal solution to (P2.2) satisfies the rank-one constraint, the optimal beamforming vector, $\mathbf{f}$, can be obtained by performing eigenvalue decomposition (EVD)

$$\Gamma \triangleq \sum_{k=1}^{K} \log\left(1+\frac{\alpha_k|\mathbf{g}_k^H\mathbf{h}_{T_k}^b|^2\mathrm{Tr}\left((\mathbf{h}_{T_k}^f)^T\mathbf{F}\mathbf{h}_{T_k}^f\right)}{\sum_{j\neq k}^{K}\alpha_j|\mathbf{g}_k^H\mathbf{h}_{T_j}^b|^2\mathrm{Tr}\left((\mathbf{h}_{T_j}^f)^T\mathbf{F}\mathbf{h}_{T_j}^f\right)+\beta\mathrm{Tr}\left(\mathbf{g}_k^H\mathbf{H}_{\mathrm{SI}}\mathbf{F}\mathbf{H}_{\mathrm{SI}}^H\mathbf{g}_k\right)+\frac{\sigma_R^2}{P_T}\|\mathbf{g}_k\|^2}\right). \tag{7}$$

$$B_k\left(\mathbf{F},\mathbf{F}^o\right)=\log\left(\sum_{j\neq k}\alpha_j|\mathbf{g}_k^H\mathbf{h}_{T_j}^b|^2\mathrm{Tr}\left((\mathbf{h}_{T_j}^f)^T\mathbf{F}^o\mathbf{h}_{T_j}^f\right)+\beta\mathrm{Tr}\left(\mathbf{g}_k^H\mathbf{H}_{\mathrm{SI}}\mathbf{F}^o\mathbf{H}_{\mathrm{SI}}^H\mathbf{g}_k\right)+\frac{\sigma_R^2}{P_T}\|\mathbf{g}_k\|^2\right)$$
$$+\mathrm{Tr}\left(\mathbf{F}-\mathbf{F}^o\right)\times\frac{\sum_{j\neq k}\alpha_j|\mathbf{g}_k^H\mathbf{h}_{T_j}^b|^2\mathrm{Tr}\left((\mathbf{h}_{T_j}^f)^T\mathbf{h}_{T_j}^f\right)+\beta\mathrm{Tr}\left(\mathbf{g}_k^H\mathbf{H}_{\mathrm{SI}}\mathbf{H}_{\mathrm{SI}}^H\mathbf{g}_k\right)}{\sum_{j\neq k}\alpha_j|\mathbf{g}_k^H\mathbf{h}_{T_j}^b|^2\mathrm{Tr}\left((\mathbf{h}_{T_j}^f)^T\mathbf{F}^o\mathbf{h}_{T_j}^f\right)+\beta\mathrm{Tr}\left(\mathbf{g}_k^H\mathbf{H}_{\mathrm{SI}}\mathbf{F}^o\mathbf{H}_{\mathrm{SI}}^H\mathbf{g}_k\right)+\frac{\sigma_R^2}{P_T}\|\mathbf{g}_k\|^2}, \tag{9}$$

$$A_k=\sum_{i=1}^{K}\alpha_i|\mathbf{g}_k^H\mathbf{h}_{T_i}^b|^2\mathrm{Tr}\left((\mathbf{h}_{T_i}^f)^T\mathbf{F}\mathbf{h}_{T_i}^f\right)+\beta\mathrm{Tr}\left(\mathbf{g}_k^H\mathbf{H}_{\mathrm{SI}}\mathbf{F}\mathbf{H}_{\mathrm{SI}}^H\mathbf{g}_k\right)+\frac{\sigma_R^2}{P_T}\|\mathbf{g}_k\|^2. \tag{10}$$

Algorithm 1 Iterative Algorithm for Precoder Optimization

1: Input: Set $it=1$, initial $\mathbf{f}^{(it)}$, and $(\mathbf{F}^o)^{(it)}=\mathbf{f}^{(it)}\ \mathbf{f}^{H^{(it)}}$.
2: **while** (8a) does not converge **do**
3: Solve (8a) to derive $\mathbf{F}^{(it)}$.
4: Update $(\mathbf{F}^o)^{(it)}\leftarrow\mathbf{F}^{(it)}$.
5: $it=it+1$;
6: **end while**
7: **Return** $\mathbf{F}^{*(it)}$ where $\mathbf{f}^\star$ is simply the eigenvector corresponding to the non-zero eigenvalue of $\mathbf{F}^{*(it)}$.

over $\mathbf{F}^*$. It can be shown that $\mathbf{F}^*$ satisfies the rank-one. A similar proof can be found in [12].

B. Optimization Over Combiner $\mathbf{g}_k$

Since the corresponding SINR of each tag observed at the $\mathbf{R}$ depends on its associate combiner vector, we maximize the sum rate by optimizing the SINR of each tag individually. Accordingly, we have

$$\text{(P3)}: \quad \max_{\mathbf{g}_k} \quad \gamma_k, \tag{11a}$$
$$\text{s.t.} \quad \|\mathbf{g}_k\|^2=1,\ \forall k. \tag{11b}$$

By rewriting the objective function in (11a), we get the following optimization problem:

$$\text{(P3.1)}: \quad \max_{\mathbf{g}_k} \quad \frac{\mathbf{g}_k^H\mathbf{h}_{T_k}^b(\mathbf{h}_{T_k}^b)^H\mathbf{g}_k}{\mathbf{g}_k^H\mathbf{Q}\mathbf{g}_k}, \tag{12a}$$
$$\text{s.t.} \quad \|\mathbf{g}_k\|^2=1,\ \forall k, \tag{12b}$$

where

$$\mathbf{Q}=\mathbf{I}_N+\frac{P_T}{\sigma_R^2}\left(\sum_{j\neq k}\alpha_j\mathbf{h}_{T_j}^b(\mathbf{h}_{T_j}^b)^H|(\mathbf{h}_{T_j}^f)^T\mathbf{f}|^2+\beta\mathbf{H}_{\mathrm{SI}}\mathbf{F}\mathbf{H}_{\mathrm{SI}}^H\right). \tag{13}$$

It can be noticed that (12a) is a well-known Rayleigh quotient maximization problem [5], [6], and its optimal value is given by

Algorithm 2 Iterative Algorithm for reflection coefficients Optimization

1: Input: Set $it=1$, tolerance $\epsilon>0$, initial $\alpha_k^{(it)}$, given $\mathbf{f}$ and $\mathbf{g}_k$, initial guess of SINR, $\hat{\gamma}_m^{(it)}$.
2: **while** $\max_{m\in K}|\gamma_m^*-\hat{\gamma}_m^{(it)}|\geq\epsilon$ **do**
3: Solve (16a) to obtain $\alpha_k^{(it)}$ and γ_m^*.
4: Update $\hat{\gamma}_m^{(it)}\leftarrow\gamma_m^*$.
5: $it\leftarrow it+1$;
6: **end while**
7: **Return** $\alpha_k^{*(it)}$.

$$\mathbf{g}_k^*=\frac{\mathbf{Q}^{-1}\mathbf{h}_{T_k}^b}{\|\mathbf{Q}^{-1}\mathbf{h}_{T_k}^b\|},\ k\in\mathcal{K}. \tag{14}$$

C. Optimization Over α_k

As the objective function (4a) is a linear-fractional function of α_k, it is a pseudolinear (both pseudoconvex and pseudoconcave) with respect to α_k [5]. However, the sum rate problem in (4a) does not preserve the pseudolinearity property. Thus the globally optimal values cannot be achieved. Nevertheless, it can be represented as a conventional power allocation problem. Then, we can recast the problem as below:

$$\text{(P4)}: \quad \min_{\gamma_m,\alpha_k} \quad \sum_{m=1}^{K}\log(1+\gamma_m), \tag{15a}$$
$$\text{s.t.} \quad \gamma_k>\gamma_m, \tag{15b}$$
$$\text{(4d), (4c)},\ \forall k, \tag{15c}$$

where γ_m is a slack variable. By considering that the objective of (15) is an increasing function over γ_m, and also $\log(\cdot)$ is a monotonically increasing function, it can be reformulated equivalently as $\min_{\gamma_m,\alpha_k}\prod_{m=1}^{K}(1+\gamma_m)^{-1}$. We note that the constraints of (P4) are posynomial functions. Therefore, if the objective is a monomial or posynomial function, (P4) becomes a GP, which is a convex problem [15, Lemma 1]. As a result, (P4) is reformulated as follows:

Algorithm 3 Iterative AO for Sum Rate Maximization

1: Input: Set $it = 1$, tolerance $\epsilon > 0$, initial $\alpha_k^{(it)}$, $\mathbf{f}^{(it)}$, and $R_S^{(it)} = 0$.
2: **Do** ▷ Iteration
3: Solve (12a) to derive $\mathbf{g}_k^{*(it)}$.
4: Run Algorithm 1 to obtain $\mathbf{f}^{*(it)}$.
5: Run Algorithm 2 to obtain $\alpha^{*(it)}$.
6: Set $R_s^{(it)} = \sum_{k=1}^{K} R_k$.
7: $it \leftarrow it + 1$;
8: **While** $|R_s^{(it)} - R_s^{(it-1)}| \geq \epsilon$ ▷ Termination
9: **Return** $\mathbf{g}_k^{*(it)}$, $\mathbf{f}^{*(it)}$, and $\alpha_k^{*(it)}$.

$$\text{(P4.1)}: \quad \max_{\gamma_m, \alpha_k} \quad \prod_{m=1}^{K} \gamma_m^{-\frac{\hat{\gamma}_m}{1+\hat{\gamma}_m}}, \tag{16a}$$

$$\text{s.t.} \quad \gamma_k > \gamma_m, \ \forall k, \tag{16b}$$

$$\nu^{-1}\hat{\gamma}_m < \gamma_m \leq \nu\hat{\gamma}_m, \tag{16c}$$

$$\text{(4d), (4c)}, \ \forall k, \tag{16d}$$

where $\hat{\gamma}_m$ denotes the initial guess for the required SINR of each user which can be obtained by substituting an initial precoder, combiners, and reflection coefficients into (3). Besides, $\nu > 1$ controls the desired approximation accuracy and the convergence speed as in each entry. Reference [15] shows that $\nu = 1.1$ obtains a trade-off between accuracy and convergence speed in most practical cases. Problem (P4.1) is a GP problem that can be solved efficiently by using CVX [14]. Algorithm 2 represents the detailed steps to return optimal α_k. Ultimately, the overall AO algorithm is represented in Algorithm 3.

D. Complexity Analysis

The complexity of the proposed algorithm can be assessed as follows. To compute $\mathbf{f}^{(it)}$ which is in the from of standard SDR problem, the complexity can be calculated as $C_1 = \mathcal{O}(I_1(2K(N_t^2) + N_t + N_r)^{4.5})$, where I_1 is the number of iterations for converge. The complexity of the precoder vectors by considering the inverse computational complexity of a matrix is given by $C_2 = \mathcal{O}\left(K(K(N_r^2 + N_t))^3\right)$. Also, the complexity of solving the GP algorithm is given by $C_3 = \mathcal{O}(I_2 K^{3.5})$, where I_2 is the number of iterations to converge to its optimal value. Finally, the overall computational complexity of the Algorithm 3 is $\mathcal{O}\left(I_{it}(C_1 + C_2 + C_3)\right)$, where I_{it} is the required number of iteration for the outer algorithm to converge.

V. Numerical Results and Discussion

This section evaluates the performance of the proposed transceiver design of beamformers and the optimization of the reflection coefficients. Comparisons are thus made between the sum rate of Algorithm 3 and that of the three following benchmarks:

1) Baseline 1 omits the EH constraint (4c) of Algorithm 3.
2) Baseline 2 omits RSI constraint (4b) from Algorithm 3.
3) Baseline 3 solves Algorithm 3 without EH constraint (4c) and by using random reflection coefficients at the tags.

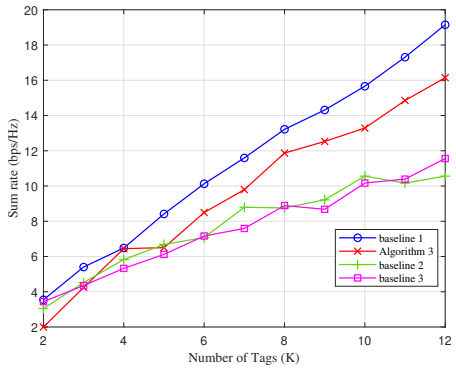

Fig. 2: Sum rate versus the number of tags, K, with $N_t = N_r = K + 2$.

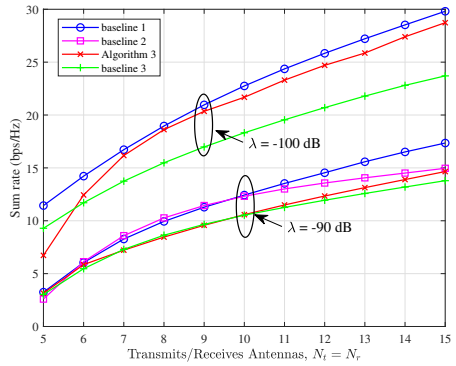

Fig. 3: Sum rate versus the number of transmit/receive antennas.

Unless otherwise specified, the simulation parameters are set as follows: $K = 5$, $N_T = N_R = 7$, $P_T = 30$ dBm, $\sigma_n^2 = -120$ dBm, $\rho = 0$, $\epsilon = 10^{-3}$, $\eta = 0.4$, $\beta = 10^{-9}$, $P_{\text{th}} = 1$ μw, $\lambda = -90$ dB, $r^2 = 100$ m^2, and $\bar{K} = 0$ dB. The path-loss between the $\mathbf{R}$ and $\mathbf{T}_k$, $k \in \mathcal{K}$, is defined as $\xi_{T_k}^j = \left(\frac{3\times10^8}{4\text{f}\pi}\right)^2 d_k^{-\varrho}$, where $j \in \{f, b\}$, f = 915 MHz is the carrier frequency, $\varrho = 2$ is the path-loss exponent, and d_k is the distance from the $\mathbf{R}$ to $\mathbf{T}_k$, $k \in \mathcal{K}$. The simulations are based on averaging over 10^3 Monte Carlo iterations.

Fig. 2 shows the impact of the number of tags, K, on the sum rate. It is vital to mention that the number of antennas should exceed the number of tags to separate tag data spatially using the linear decoding vectors $\mathbf{g}_k$ and to satisfy the EH and RSI constraints. We thus set $N_t = N_r = K + 2$, which provides the necessary spatial degrees of freedom (DoF). We expect the increased number of tags to increase the sum rate for all schemes. However, Algorithm 3 outperforms baselines two and three for over five tags. This gain results from the following reasons. First, baseline two removes the RIS constraint and operates without RSI suppression. Thus, the RSI dominates and degrades the sum throughput. Second, baseline three does not optimize the tag reflection coefficients.

There is a relatively large gap between baseline 2 and baseline 3 with baseline 1 and Algorithm 3, and the gap increases with the number of tags. Hence, we conclude that the

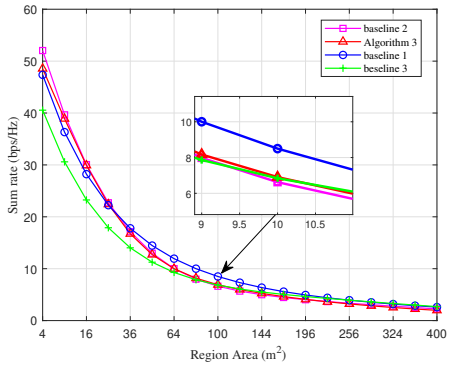

Fig. 4: Sum rate versus region area, $r \times r$, for different baseline schemes.

proposed optimization yields substantial gains over baseline 2 and 3. Baseline 1, compared to Algorithm 3, is the price to pay for supporting tags with their required power. This fact shows the non-negligible impact of the RSI. Recall that tags are assumed to have enough power to perform their reflections in baseline 1 and thus do not perform EH. Therefore, this baseline releases some of the spatial DoFs that would have been utilized to ensure the tags meet the EH threshold. Thus, it suppresses the RSI effect more effectively and achieves a higher sum rate. However, when tags are running on low power, replacing their batteries is not cost-effective and is sometimes impossible (e.g., in toxic industrial regions). Therefore, EH from the $\mathbf{R}$ keeps the tag's operation. As a result, the proposed design can fairly compete and gain near results to baseline one.

Fig. 3 presents the performance comparison of the sum rate obtained by Algorithm 3 accompanying other baselines for the diverse number of transmit/receive antennas (N_t/N_r) by considering two different values for λ. This figure shows the superiority of our proposed design when RSI is strictly limited, say $\lambda = -100$ dB, compared to baseline 2 and baseline 3. As RSI's power is reduced more, better performance in terms of sum rate is achievable. Increasing the number of antennas at the $\mathbf{R}$ has a direct impact on the improvement of the sum rate as the system exploits the array gain in the downlink transmission and multiplexing gain in the uplink. For $\lambda = -90$ dB, the proposed design can only obtain a higher gain than baselines 2 and 3 for the number of antennas greater than 15. Thus, Algorithm 3 excels other schemes for a higher number of antennas.

Fig. 4 represents the impact of the coverage area for different schemes on the sum rate. As the coverage area gets bigger, there is a slight difference between schemes. However, for a small area, specifically, 4 m^2 to 25 m^2, the proposed scheme and baseline 2 have a bit more gain than other baselines since in these two schemes, tags can harvest energy, which can satisfy their required power better because of the strong forward links in short distances. Baseline 1 slightly outperforms in the moderate coverage area, 36 m^2 to 144 m^2. Because, as the area gets larger, the distance of the tag from the $\mathbf{R}$ increases. Therefore, providing the required tag's power becomes challenging while suppressing the RSI. Consequently, baseline 1 achieves more gain since it relaxes the EH constraint.

VI. Conclusion and Future Work

This paper studied a multi-tag MBS network with a MIMO reader. Since the reader operates in the FD mode, the presence of the RSI affects the system performance. This issue has not been investigated before. We thus considered a more realistic model where we represent the imperfection level of the SIC process of the reader by coefficient $\beta > 0$. Thus for finite $\beta > 0$, we developed an algorithm to limit the impact of the RSI level and enable the tags to harvest sufficient energy while maximizing the sum rate by jointly optimizing the precoder, combiners, and reflection coefficients. The algorithm based on the AO approach solves the non-convex optimization problem. The results showed the crucial effect of controlling RSI along satisfying adequate power for tags while providing a robust sum rate. The proposed design often yielded a better sum rate than the baselines.

References

[1] H. Stockman, "Communication by means of reflected power," *Proceedings of the IRE*, vol. 36, pp. 1196–1204, 1948.

[2] F. Rezaei, C. Tellambura, and S. P. Herath, "Large-scale wireless-powered networks with backscatter communications - A comprehensive survey," *IEEE Open J. Commun. Soc.*, vol. 1, pp. 1100–1130, 2020.

[3] M. L. Memon, N. Saxena, A. Roy, and D. R. Shin, "Backscatter communications: Inception of the battery-free era—A comprehensive survey," *Electronics*, vol. 8, no. 2, p. 129, 2019.

[4] D. P. Villame and J. S. Marciano, "Carrier suppression locked loop mechanism for UHF RFID readers," in *IEEE International Conference on RFID (IEEE RFID 2010)*, pp. 141–145, IEEE, 2010.

[5] D. Mishra and E. G. Larsson, "Sum throughput maximization in multi-tag backscattering to multiantenna reader," *IEEE Trans. Commun.*, vol. 67, no. 8, pp. 5689–5705, 2019.

[6] G. Sacarelo and Y. H. Kim, "Beamforming and reflection coefficient control for multiantenna backscatter communication with non-orthogonal multiple access," *IEEE Access*, vol. 9, pp. 56104–56114, 2021.

[7] A. Al-Nahari, R. Jäntti, D. Mishra, and J. Hämäläinen, "Massive MIMO beamforming in monostatic backscatter multi-tag networks," *IEEE Commun. Lett.*, vol. 25, no. 4, pp. 1323–1327, 2021.

[8] W. Ma, W. Wang, and T. Jiang, "Joint energy harvest and information transfer for energy beamforming in backscatter multiuser networks," *IEEE Trans. Commun.*, vol. 69, no. 2, pp. 1317–1328, 2021.

[9] S. Gong, Y. Zou, D. T. Hoang, J. Xu, W. Cheng, and D. Niyato, "Capitalizing backscatter-aided hybrid relay communications with wireless energy harvesting," *IEEE Internet Things J.*, vol. 7, no. 9, pp. 8709–8721, 2020.

[10] X. Lu, H. Jiang, D. Niyato, D. I. Kim, and Z. Han, "Wireless-powered device-to-device communications with ambient backscattering: Performance modeling and analysis," *IEEE Trans. Wirel. Commun.*, vol. 17, no. 3, pp. 1528–1544, 2018.

[11] G. Yang, C. K. Ho, and Y. L. Guan, "Multi-antenna wireless energy transfer for backscatter communication systems," *IEEE J. Sel. Areas Commun.*, vol. 33, no. 12, pp. 2974–2987, 2015.

[12] S. Zargari, A. Khalili, Q. Wu, M. Robat Mili, and D. W. K. Ng, "Max-min fair energy-efficient beamforming design for intelligent reflecting surface-aided SWIPT systems with non-linear energy harvesting model," *IEEE Trans. Veh. Technol*, vol. 70, no. 6, pp. 5848–5864, 2021.

[13] Y. Dai and X. Dong, "Power allocation for multi-pair massive MIMO two-way AF relaying with linear processing," *IEEE Trans. Wirel. Commun.*, vol. 15, no. 9, pp. 5932–5946, 2016.

[14] M. Grant and S. Boyd, "CVX: Matlab software for disciplined convex programming, version 2.1," 2014.

[15] P. C. Weeraddana, M. Codreanu, M. Latva-aho, and A. Ephremides, "Resource allocation for cross-layer utility maximization in wireless networks," *IEEE Trans. Veh. Technol.*, vol. 60, no. 6, pp. 2790–2809, 2011.